Supporting Information

Arias-Cartin et al. 10.1073/pnas.1010427108

SI Text

NarGHI Purification. Inner membrane vesicles (IMVs) were solubilized with 1% n-dodecyl-β-D-maltoside (DDM) overnight at 4 °C in 20 mM Mes pH 6.5. The soluble fraction was centrifuged at 100,000 × *g* for 30 min. The supernatant was loaded onto a Mono Q 10/100 column (GE Healthcare), and the protein was eluted in a 50 mM Mes pH 6.5, 0.03% DDM, 10% (vol/vol) glycerol buffer with a linear gradient of NaCl. NarGHI-enriched fractions were pooled and dialyzed (50 KDa MCWO SpectraPor) overnight at 4 °C against buffer A [50 mM Tris-HCl pH 7.5, 10% (vol/vol) glycerol and 0.03% DDM or 0.15% DDM]. After dialysis, the purified sample was loaded onto a Mono Q 10/100 column equilibrated with buffer A plus 100 mM NaCl and eluted as described before. Peak fractions containing nitrate reductase of at least ≥98% purity as judged on the basis of SDS-PAGE analysis were pooled, concentrated, and dialyzed using 50 mM Tris-HCl pH 7.5, EDTA 5 mM, glycerol 5%.

Nitrate Reductase Activity. Nitrate reductase activity was measured with standard assays using either artificial benzyl viologen (1) or quinol analogs such as menadiol or decyl-ubiquinol as electron donors (2). Although the use of reduced benzyl viologen as electron donor allows estimation of the structural and functional integrity of the NarGH component, the use of quinol analogs allows the estimation of the electron flow from the quinol-oxidizing site within NarI to the nitrate-reducing site in NarG and thus reflects the physiological electron pathway throughout the NarGHI complex. Assessment of the quality and integrity of the purified NarGHI complex has thus been addressed by using all three electron donors. Although identical results were obtained using either of the two quinol analogs, menadiol and decyl-ubiquinol, we only provided herein data for menadiol for simplicity. As shown in Table 2, a dramatic loss of quinol oxidase activity is observed using 0.15% of DDM, which contrasts with the less pronounced effect on the benzyl viologen activity as expected. Finally, the benzyl viologen activity of the purified NarGHI complex approximates the value obtained for the soluble NarGH complex (3).

As a control, the effect of DDM on quinol oxidase activity of the purified NarGHI complex has been assessed (Fig. S2). Purified NarGHI samples (using either 0.03 or 0.15% of DDM) were incubated for 5 min at 37 °C in the reaction medium with increasing DDM concentration before initiation of the reaction. A reduction of the menadiol activity was only observed when the final concentration of DDM reached 0.08%, a value which is several orders of magnitude above the concentration of DDM present in our activity assays (never exceeding 0.0001%). Accordingly, the presence of low amounts of DDM has no influence on the estimation of the quinol:nitrate oxidoreductase activity.

Lipids extraction and Thin-Layer Chromatography (TLC) analysis. DDM in purified NarGHI was eliminated by incubation with 240 mg of Bio-Beads (BioRad, SM2) for 1 h at room temperature. Subsequently, the protein sample was lyophilized (approximately 10 mg) in glass tubes and resuspended in 3 mL of $HCCl_3$/CH_3OH (2:1). Suspensions were vortexed for 1 min and stirred for 6 h at room temperature. Then, 115 μL of NH_4OH 25% was added and stirred 1 d more, this procedure was repeated once, and 1 mL of H_2O was added at the end of this step. Samples were agitated for 1 min and let without agitation for 1 h; 0.5 mL of H_2O was added again and let for phase formation. Samples were centrifuged at 2,000 × *g* for 5 min, and organic phase was extracted, evaporated with an argon flux, and kept at −20 °C until analysis. Extracted lipids were resuspended with 200 μL of $HCCl_3$ and applied to a silica gel 60 TLC plate (10 × 20 cm, Merck) with a TLC Sampler (CAMAG). Samples were resolved using $HCCl_3$/CH_3OH/CH_3COOH mixture (65:25:4). After spraying the plates with a cupric acetate phosphoric acid solution, lipid bands were revealed by heating the plates at 180 °C for 10–15 min. Quantification was performed using a densitometric TLC scanner (CAMAG) and pure phospholipids standards (Avanti Lipids).

Growth of the PE-Deficient Strain. The bacterial strain AD93/pDD72 was routinely grown at 30 °C in LB media (4) (Table S3). Plasmid pDD72 is used as the source of functional *pss* gene product at 30 °C but not at 43 °C thanks to the presence of a thermosensitive origin of replication. The strain was transformed with the pVA700 plasmid allowing overexpression of the NarGHI complex (5). Curing of the pDD72 was performed essentially as described in ref. 6. A strain carrying a null allele of *pssA* completely lacks PE and is only viable when supplemented with divalent cations. The resulting AD93/pVA700 strain was immediately used for semianaerobic growth using an LB media supplemented with 50 mM of $MgCl_2$. NarGHI-enriched membranes were prepared as described before (7) and assayed for both benzyl viologen and quinol activities.

EPR Quantitation of the NarGHI Hemes. Quantitation of the heme b_D content was achieved relatively to the nitrate reductase heme b_P content in each enzyme preparation to get rid of the differences in the concentration level of NarGHI in the different preparations. For this purpose, a fourth-order polynomial baseline correction was first applied to the experimental spectrum showing the low field features of the heme EPR signals to get rid of baseline artefacts coming from free Fe(III) ions ($g \sim 4.3$) in the samples. The low field feature of the heme b_D EPR signature was resolved into two components modeled by two normalized Gaussian absorption line shapes with full widths at half height of 1.25 and 0.75 mT for the $g \sim 3.35$ and the $g \sim 3.20$ components, respectively. These linewidths are due to *g*-strain effects (8) and indicate an increase of structural microheterogeneity of heme b_D upon delipidation. Their respective amplitudes were then optimized so that their sum optimally fitted the experimental spectrum. Using this procedure, the uncertainty on the ratio between the two forms of the heme b_D was estimated at about 10%. Quantitative analysis of the heme b_D EPR signals thus reveals that the relative proportion of the $g \sim 3.35$ and the $g \sim 3.20$ features increases from 2.3 in NarGHI-enriched IMVs to 3.6 and 4.3 in NarGHI purified with 0.03% DDM and with 0.15% DDM, respectively.

Moreover, as the area under the low field peaks of hemes was shown to be proportional to the spin intensity of the whole anisotropic EPR spectrum (9), the spin intensity corresponding to the heme b_D EPR signal taking into account the two components could be compared with that of heme b_P. The corresponding ratio did not change by more than approximately 15% in the above-mentioned enzyme preparations, which shows that the relative content of the two hemes b_P and b_D is unchanged. Given the accuracy of the quantitation method, our data are consistent with an interconversion of the $g \sim 3.20$ species into that with $g \sim 3.35$ consecutive to the delipidation process.

1. Jones RW, Garland PB (1977) Sites and specificity of the reaction of bipyridylium compounds with anaerobic respiratory enzymes of *Escherichia coli*. Effects of permeability barriers imposed by the cytoplasmic membrane. *Biochem J* 164:199–211.
2. Giordani R, Buc J, Cornish-Bowden A, Cardenas ML (1997) Kinetic studies of membrane-bound nitrate reductase A from *Escherichia coli* with menadiol and duroquinol, analogues of physiological electron donors. *Eur J Biochem* 250:567–577.
3. Buc J, et al. (1995) Kinetic studies of a soluble alpha beta complex of nitrate reductase A from *Escherichia coli*. Use of various alpha beta mutants with altered beta subunits. *Eur J Biochem* 234:766–772.
4. DeChavigny A, Heacock PN, Dowhan W (1991) Sequence and inactivation of the pss gene of *Escherichia coli*. Phosphatidylethanolamine may not be essential for cell viability. *J Biol Chem* 266:5323–5332.
5. Guigliarelli B, et al. (1996) Complete coordination of the four Fe-S centers of the beta subunit from *Escherichia coli* nitrate reductase. Physiological, biochemical, and EPR characterization of site-directed mutants lacking the highest or lowest potential [4Fe-4S] clusters. *Biochemistry* 35:4828–4836.
6. Mikhaleva NI, Santini CL, Giordano G, Nesmeyanova MA, Wu LF (1999) Requirement for phospholipids of the translocation of the trimethylamine N-oxide reductase through the Tat pathway in *Escherichia coli*. *FEBS Lett* 463:331–335.
7. Lanciano P, Vergnes A, Grimaldi S, Guigliarelli B, Magalon A (2007) Biogenesis of a respiratory complex is orchestrated by a single accessory protein. *J Biol Chem* 282:17468–17474.
8. More C, Gayda JP, Bertrand P (1990) Simulations of the *g*-strain broadening of low-spin hemoprotein EPR spectra based on the t_{2g} hole model. *J Magn Reson* 90:486–499.
9. Aasa R, Vanngard T (1975) EPR signal intensity and powder shapes: A reexamination. *J Magn Reson* 19:308–315.
10. Potter LC, Millington P, Griffiths L, Thomas GH, Cole JA (1999) Competition between *Escherichia coli* strains expressing either a periplasmic or a membrane-bound nitrate reductase: Does Nap confer a selective advantage during nitrate-limited growth? *Biochem J* 344:77–84.
11. Datsenko KA Wanner BL (2000) One-step inactivation of chromosomal genes in *Escherichia coli* K-12 using PCR products. *Proc Natl Acad Sci USA* 97:6640–6645.
12. Guigliarelli B, et al. (1992) EPR and redox characterization of iron-sulfur centers in nitrate reductases A and Z from *Escherichia coli*. Evidence for a high-potential and a low-potential class and their relevance in the electron-transfer mechanism. *Eur J Biochem* 207:61–68.

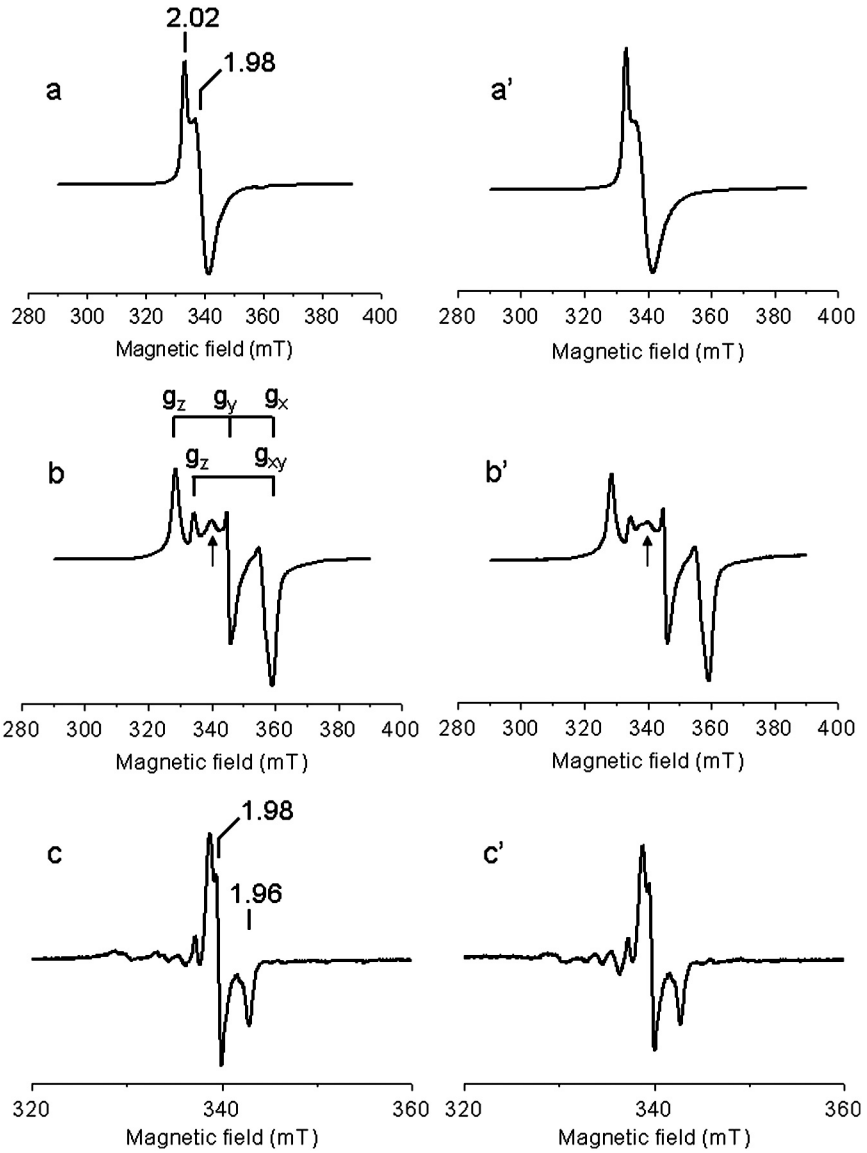

Fig. S1. Representative spectra of the redox centers present in NarGHI upon progressive delipidation. X-band EPR spectra around $g = 2$ of redox-poised NarGHI in NarGHI-enriched IMVs (*a*–*c*) and NarGHI-DDM solubilized with 0.15% DDM (*a*′–*c*′). Spectra *a* and *a*′ show the FS4 EPR spectrum in oxidized samples redox-poised at +398 mV (*a*) and +400 mV (*a*′) using potassium ferricyanide. Spectra *b* and *b*′ show the FeS clusters in partially reduced samples redox-poised at −105 mV (*c*) and −109 mV (*c*′) using sodium dithionite. These potentials were chosen to illustrate spectra of samples in which both FS1 and FS3 are reduced. The spectrum of FS1 was simulated by Guigliarelli et al. as the sum of two components, a major rhombic component with $g_z = 2.05$, $g_y = 1.95$, $g_x = 1.88$ and a minor axial component with $g_z = 2.01$, $g_{xy} = 1.88$ (12). The contribution of FS3 is indicated by a vertical arrow. Spectra *c* and *c*′ show the nearly axial Mo(V) EPR signal in samples prepared at +199 mV (*b*) and +195 mV (*b*′). EPR conditions for FeS and Mo(V): temperature, 12.5 and 50 K; microwave power, 100 and 4 mW at 9.41 GHz; modulation amplitude, 0.5 and 0.4 mT at 100 kHz, respectively.

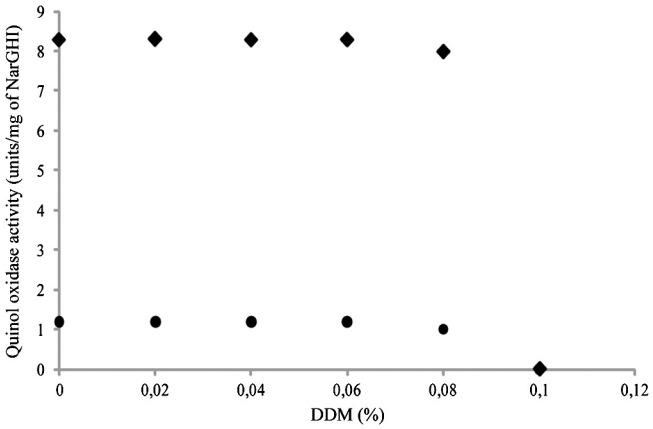

Fig. S2. Effect of DDM on quinol oxidase activity of NarGHI. Purified NarGHI samples were incubated for 5 min at 37 °C in the quinol oxidase reaction medium with increasing DDM concentration before initiation of the reaction by nitrate. The resulting quinol oxidase values herein indicated are expressed in μmoles of oxidized quinol/ min /mg of purified NarGHI and represent the mean of three independent measurements. The samples used are purified NarGHI with 0.03% of DDM (filled diamonds) or with 0.15% of DDM (filled circles).

Table S1. Redox potential of individual metal centers of NarGHI-enriched IMVs or DDM-isolated enzyme

	Hemes (±10 mV)		[3Fe-4S]	Mo(V)
	b_D	b_P	(±20 mV)	
Membrane	−15	+100	+180	+160
DDM 0.03%	−10	+130	+180	+160
DDM 0.15%	0	+80	+180	+150

Values were obtained by redox titration experiments monitored by EPR spectroscopy. EPR conditions for FeS and Mo(V): temperature, 12.5 and 50 K; microwave power, 100 and 4 mW at 9.41 GHz; modulation amplitude, 0.5 and 0.4 mT at 100 kHz, respectively. EPR conditions for hemes are given in the caption of Fig. 3.

Table S2. Quinol:nitrate oxidoreductase activity in IMVs with either plasmidic expression (recombinant) or chromosomal expression (chromosomal) of NarGHI

	Recombinant	Chromosomal
NarGHI, %	27.6 ± 1.3	3.1 ± 0.5
Activity, U/mg	18.7 ± 1.3	42.6 ± 1.6

Cells were grown under anaerobic conditions in LB media supplemented with glucose (0.3%) and nitrate (0.2%). The percentage of NarGHI present in the IMVs issued from anaerobically grown BW25113 cells (indicated as NarGHI, %) has been measured by immunoelectrophoresis using antisera directed against NarGHI. The quinol oxidase activity has been measured as described in *Materials and Methods*.

Table S3. Bacterial strains and plasmids

Strains/plasmids	Description	Source
Strains		
JCB4023	RK4353 *narG*::ery Δ*napA narZ*::Ω Spc^R	ref. 10
BW25113	*lacI*^{q}*rrnB*$_{T14}$Δ*lacZ*$_{W16}$*hsdR*514 Δ*araBAD*$_{AH33}$Δ*rhaBAD*$_{LD78}$	ref. 11
AD93	*pss*93 :: *kan recA srl* :: Tn10 *nadB*$^+$	ref. 4
Plasmids		
pVA700	pJF119EH, NarGHJI, Amp^R	ref. 5
pRAC	pGEM-T, NarJI, Amp^R	this work
pVA700-W162A	pJF119EH, NarGHJI$_{W162A}$, Amp^R	this work
pDD72	*pss*$^+$ *cam* (derivative of pMT101)	ref. 4

Table S4. Primers used for site-directed mutagenesis

Primer	Sequence	Source
NarIW162A_1	5′-GTTGGCGCAGCGCAGTCGGTGGTGACCTTC-3′	this work
NarIW162A_2	5′-CTGCGTTGCGCCAACCAGTTTCATCATCTC-3′	this work